

Producing Highly Predictive Qsar Models Of Benzimidazole Derivatives As Potent Antifungal Agents

Rani S. Kankate^{1*}, Sampada L. Deshmukh², Ziyaul Haque³, Eknath D. Ahire⁴, Sanjay J. Kshirsagar⁵

¹Assistant Professor, Department of Pharmaceutical Chemistry, MET's Institute of Pharmacy, Bhujbal Knowledge City, Adgaon, Nashik 422003, Maharashtra, India

^{2,3}Department of Pharmaceutical Chemistry, MET's Institute of Pharmacy, Bhujbal Knowledge City, Adgaon, Nashik 422003, Maharashtra, India

⁴Assistant Professor, Department of Pharmaceutics, MET's Institute of Pharmacy, Bhujbal Knowledge City, Adgaon, Nashik 422003, Maharashtra, India

⁵Professor and Principal, Department of Pharmaceutics, MET's Institute of Pharmacy, Bhujbal Knowledge City, Adgaon, Nashik 422003, Maharashtra, India

*Corresponding Authors: Dr. Rani S. Kankate, Assistant Professor

*Department of Pharmaceutical Chemistry, MET's Institute of Pharmacy, Bhujbal Knowledge City, Adgaon, Nashik 422003, Maharashtra, India E-mail: ranipharmacy@gmail.com
DOI: 10.47750/pnr.2023.14.502.267

Abstract

The antifungal efficacy of freshly synthesized Aryl Benzimidazole derivatives was investigated using quantitative structure-activity relationship (QSAR) analysis. Molecular Design Suite was used to create the statistically significant 2D-QSAR models ($r^2 = 0.8361$; $q^2 = 0.7457$; $F \text{ test} = 35.71$; $r^2_{se} = 0.0883$; $q^2_{se} = 0.1100$; $\text{pred } r^2 = 0.6511$; $\text{pred } r^2_{se} = 0.2360$). (VLifeMDS 4.3.1) The data set for the study consisted of 36 chemicals, and the training and test sets were created using the sphere exclusion (SE) algorithm, random selection, and manual selection techniques. The QSAR models were constructed using multiple linear regression (MLR) methodologies and the stepwise (SW) forward-backward variable selection method. To investigate the substitutional requirements for the favorable antifungal activity against *Candida albicans* and to provide useful information in the characterization and differentiation of their binding sites, the results of the 2D-QSAR models were further compared with 3D-QSAR models produced by kNN-MFA (kNearest Neighbor Molecular Field Analysis). The findings could help with future designs for synthesizing aryl benzimidazole derivatives of benzimidazole.

Keywords: 2D QSAR, 3DQSAR, kNN- MFA, Benzimidazole Derivatives, Antifungal Activity, Multiple Linear Regression Analysis (MLR)

INTRODUCTION

QSAR analysis (2D and 3D):

Quantitative structure activity relationships (QSAR) are the most important applications of chemometrics giving useful information for the design of new compounds acting on a specific target. A good QSAR model both enhances our understanding of the specifics of drug action and provides a theoretical foundation for lead optimization [1]. The aim of present work is to derive some statistically significant QSAR methods two dimensional and k-nearest neighbour to the study of molecular substitution sites of interest and statistically significant QSAR models for benzimidazole derivatives as high active antifungal agents [2-4].

MATERIAL AND METHODS

2D-QSAR studies and Calculation of 2D descriptor

2D-QSAR study requires the calculation of molecular descriptors; almost six physicochemical descriptors were calculated by QSAR Plus module within VLife MDS. The invariable descriptors (descriptors that are constant for all the molecules) were removed, as they do not contribute to the QSAR. Variable selection was performed Multiple linear regression methodology [5, 6]. 2D descriptors were calculated which encoded different aspects of molecular structure and consists of electronic, thermodynamic, spatial and structural descriptors, e.g., retention index (chi), atomic valence connectivity index (chi V), path count, chain path count, cluster, path cluster, element count, estate number, semi-empirical, molecular weight, molecular refractivity, slogP, and topological index. The various alignment-independent (AI) descriptors [7] were also calculated. In this study to calculate AI descriptors, we have used following attributes, 2(double bonded atom), 3 (triple bonded atom), C, N, S, O and H and the distance range of 0–7.

The QSAR models are considered acceptable [8].if they satisfy all of the following conditions: (i) $Q^2 > 0.5$, (ii) $R^2 > 0.6$. The Q^2 value provided the statistical significance and predictability of the models, being used as a criterion of both robustness and predictive ability of the model. The high Q^2 value (for instance $Q^2 > 0.5$) suggests that the models will be appropriate for meaningful predictions [9, 10].

Standard error of estimate (smaller is better). It indicates how well the regression function predicts observed data. The low standard error of pred_r^2se , $q^2\text{se}$ and $r^2\text{se}$ shows absolute quality of fitness of the model. The generated QSAR model was validated for predictive ability inside the model by using cross validation (LOO) for q^2 and external validation pred_r^2 , which is more robust alternative method by dividing the data into training set & test set and calculating pred_r^2 . The high pred_r^2 and low pred_r^2se were show high predictive ability of the model. The values (pred_r^2 and pred_r^2se) related to external validation has put in all developed models [11, 12]. Further analysis shows that for all compounds the error (residual value) is very small. Residuals values (difference between actual and predicted activities) were found to be minimal. Smaller values of residuals show the high predictive power of QSAR models [13, 14].

3D-QSAR analysis:

kNN- MFA

kNN- MFA is novel methodology, unlike conventional QSAR regression methods; this methodology can handle nonlinear relationships of molecular field descriptors with biological activity, thus making it a more accurate predictor of biological activity [15, 16]. The kNN technique is a conceptually simple approach to pattern recognition problems¹⁴. In this method, an unknown pattern is classified according to the majority of the class memberships of its k nearest neighbours in the training set [17, 18]. The nearness is measured by an appropriate distance metric (e.g. a molecular similarity measure, calculated using field interactions of molecular structures). The standard kNN method is implemented simply as follows: (i) calculate distances between an unknown object (u) and all the objects in the training set; (ii) select k objects from the training set most similar to object u , according to the calculated distances, (iii) classify object u with the group to which a majority of the k objects belong [19]. An optimal k value is selected by the optimization through the classification of a test set of samples or by the leave-one out cross-validation [20]. The variables and optimal k values are chosen using different variable selection methods as described below.

Alignment rules

Molecular alignment was used to visualize the structural diversity in the given set of molecules. This was followed by generation of common rectangular grid around the molecules [21]. The template structure i.e. Benzimidazole was used for alignment by considering the common elements of the series as shown in Fig. 1 and 2. The reference molecule **X** is chosen high inhibitory effect which made it a valid lead molecule and therefore was chosen as a reference molecule. After optimizing, the template structure and the reference molecule were used to superimpose all molecules from the series using the template alignment method [22]. kNN-MFA method requires suitable alignment of given set of molecules after optimization; alignment was carried out by template based alignment method. Stereo view of aligned molecules in training set and test set is shown in Figure 5. Fig. 1 shows the contribution plot for the all descriptors

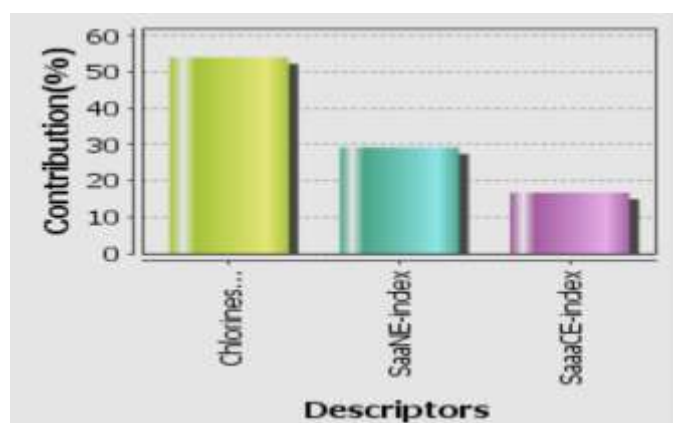


Figure 1: Contribution chart for model showing contribution of different descriptors

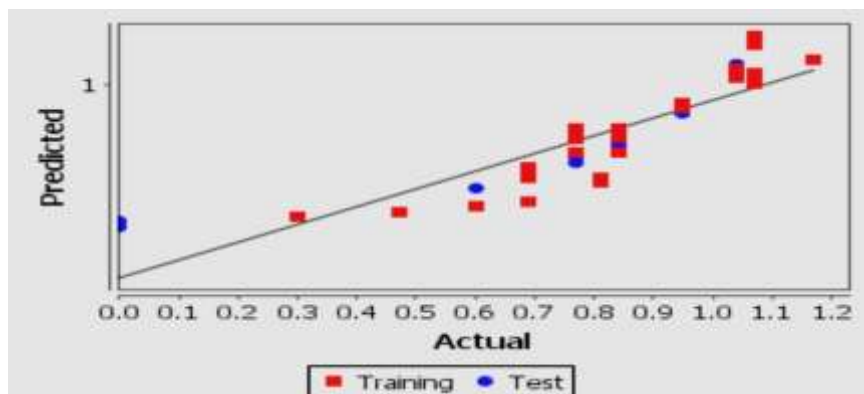


Figure 2: Data fitness plot for model

Creation of Interaction Energies

The above aligned molecules have RMSD value within a range ($<2\text{\AA}$), the molecules superimposed on template structure performed by template selection based method that is atom/shape based RMS fit, multifit [23].

Generation of training and test sets

In order to evaluate the QSAR model, data set was divided into training and test set using sphere exclusion, random selection and Manual selection method²². Training set is used to develop the QSAR model for which biological activity data are known. Test set is used to challenge the QSAR model developed based on the training set to assess the predictive power of the model which is not included in model generation [24-27].

RESULT AND DISCUSSION

QSAR analysis (2D and 3D):

The aim of present work is to derive some statistically significant QSAR methods two dimensional and k-nearest neighbour to the study of molecular substitution sites of interest and statistically significant QSAR models for benzimidazole derivatives as high active antifungal agents.

2D QSAR

In 2D QSAR analysis, multiple linear regression analysis (MLR) coupled with stepwise forward backward variable selection method was applied to generate 2D models. Selection of training and test set was done by Manual data selection and Random selection method. From these models, the one having good r^2 and pred_r^2 values was selected as best model. Statistically significant 2D QSAR models are as follows.

Model-1(Test set: 1, 13, 16, 17, 19, 23, 24, 3, 31, 5 and 9)

$$pIC_{50} = +0.3703 (\text{Chlorines Count}) + 0.6759 (\text{SaaNE-index}) + 0.7458 (\text{SaaaCE-index}) - 4.1531$$

Statistics: [n = 25; DOF = 21; $r^2 = 0.8361$; $q^2 = 0.7457$; F test = 35.71; $r^2\text{se} = 0.0883$; $q^2\text{se} = 0.1100$; $\text{pred}_r^2 = 0.6511$; $\text{pred}_r^2\text{se} = 0.2360$]

In the above QSAR equations, n is the number of molecules (Training set) used to derive the QSAR model, r^2 is the squared correlation coefficient, q^2 is the cross-validated correlation coefficient, pred_r^2 is the predicted correlation coefficient for the external test set, F is the Fisher ratio, reflects the ratio of the variance explained by the model and the variance due to the error in the regression. High values of the F-test indicate that the model is statistically significant. $r^2\text{se}$, $q^2\text{se}$ and pred_r^2se are the standard errors terms for r^2 , q^2 and pred_r^2 (smaller is better).

Interpretation of the Model

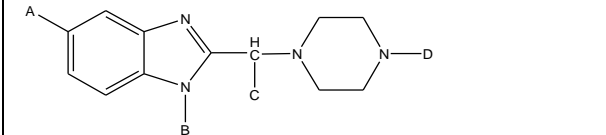
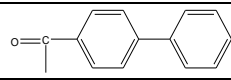
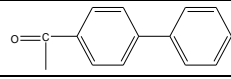
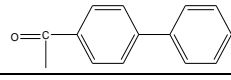
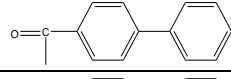
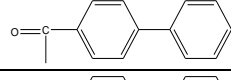
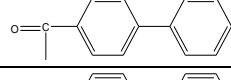
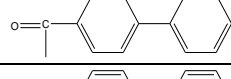
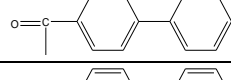
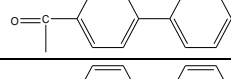
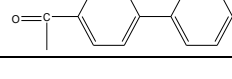
From equation, model explains 83.61% ($r^2=0.8361$) of the total variance in the training set as well as it has internal (q^2) and external (pred_r^2) predictive ability of 74.57% and 65.11% respectively. The F test shows the statistical significance of 99.99 % of the model which means that probability of failure of the model is 1 in 10000. In addition, the randomization test shows confidence of 99.9999 (Alpha Rand Pred $R^2 = 0.00000$) that the generated model is not random and hence chosen as the QSAR model. The F-test= 35.71 which is greater than the tabulated value 3.15 (Bolton 2004). From QSAR model 1 explains that, $+0.3703(\text{ChlorinesCount}) + 0.6759 (\text{SaaNE-index}) + 0.7458 (\text{SaaaCE-index}) - 4.1531$

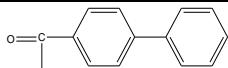
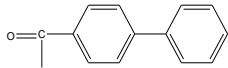
1. Positive coefficient value of ChlorinesCount [This descriptor signifies number of chlorine atoms in a compound.], on the biological activity indicated that Higher values leads to good inhibitory activity,
2. Positive coefficient value of SaaNE-index [Electrotopological state indices for number of nitrogen atom connected with two aromatic bonds.] on the biological activity indicated that Higher value leads to better inhibitory activity whereas lower value leads to decrease inhibitory activity.

3. Positive coefficient value of SaaCE-index [Electrotopological state indices for number of carbon atom connected with three aromatic bonds.] on the biological activity indicated that higher value leads to better inhibitory activity whereas lower value leads to decrease inhibitory activity. Fig. 1 shows the contribution plot for the all descriptors

Data fitness plot for model is shown in Fig.2 The plot of observed vs. predicted activity provides an idea about how well the model was trained and how well it predicts the activity of external test set. Table 1 indicating the structures of aryl benzimidazole derivatives with its activity.

Table 1: Structures of aryl benzimidazole derivatives with its activity

Sr. No.	Molecule name					Actual activity at concentration 50ug/ml (Log value)
		A	B	C	D	
1	BPC1	-H	-H	-H	-COCH ₃	0
2	BPC2	-H	-H	-CH ₃	-COCH ₃	0.47
3	BPC3	-H	-H	-Ph	-COCH ₃	0.6
4	BPC4	-H	-CH ₃	-H	-COCH ₃	0.69
5	BPC5	-H	-CH ₃	-CH ₃	-COCH ₃	0.77
6	BPC6	-H	-CH ₃	-Ph	-COCH ₃	0.77
7	BPC7	-H	-C ₂ H ₅	-H	-COCH ₃	0.84
8	BPC8	-H	-C ₂ H ₅	-CH ₃	-COCH ₃	0.84
9	BPC9	-H	-C ₂ H ₅	-Ph	-COCH ₃	0.95
10	BPC10	-Cl	-H	-H	-COCH ₃	1.07
11	BPC11	-Cl	-H	-CH ₃	-COCH ₃	1.04
12	BPC12	-Cl	-H	-Ph	-COCH ₃	1.07
13	BPC13	-H	-H	-H	-COPh	0
14	BPC14	-H	-H	-CH ₃	-COPh	0.6
15	BPC15	-H	-H	-Ph	-COPh	0.81
16	BPC16	-H	-CH ₃	-H	-COPh	0.69
17	BPC17	-H	-CH ₃	-CH ₃	-COPh	0.77
18	BPC18	-H	-CH ₃	-Ph	--COPh	0.77
19	BPC19	-H	-C ₂ H ₅	-H	-COCH ₃	0.84
20	BPC20	-H	-C ₂ H ₅	-CH ₃	-COPh	0.84
21	BPC21	-H	-C ₂ H ₅	-Ph	-COPh	0.95
23	BPC22	-Cl	-H	-H	-COPh	1.04
23	BPC23	-Cl	-H	-CH ₃	-COPh	1.04
24	BPC24	-Cl	-H	-Ph	-COPh	1.68
25	BPC25	-H	-H	-H		0.3
26	BPC26	-H	-H	-CH ₃		0.69
27	BPC27	-H	-H	-Ph		0.81
28	BPC28	-H	-CH ₃	-H		0.69
29	BPC29	-H	-CH ₃	-CH ₃		0.77
30	BPC30	-H	-CH ₃	-Ph		0.77
31	BPC31	-H	-C ₂ H ₅	-H		0.84
32	BPC32	-H	-C ₂ H ₅	-CH ₃		0.84
33	BPC33	-H	-C ₂ H ₅	-Ph		0.95
34	BPC34	-Cl	-H	-H		1.07

35	BPC35	-Cl	-H	-CH ₃		1.17
36	BPC36	-Cl	-H	-Ph		1.15

The graph of observed vs. predicted activity of training and test sets for model is shown in Fig. 3 and 4, it reveals that the model is able to predict the activity of training set quite well as well as external test set, providing confidence of model.

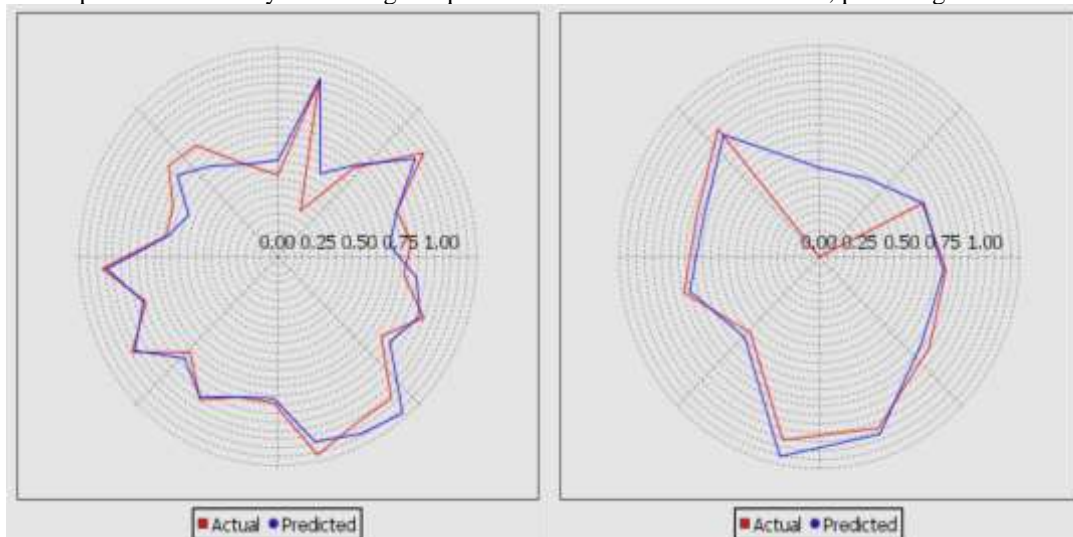


Figure 3: Training set

Figure 4: Test set

Result of the observed vs. predicted inhibitory activity for the training and test compounds for the Model 10 is shown in Table 2.

Table 2: Summary of 2D QSAR Model 1-3.

Trials	r ²	q ²	r ² se	q ² se	Pred_r ²	Pred_r ² se	F test
1(Model-1)	0.8361	0.7457	0.0883	0.1100	0.6511	0.2360	35.71
2(Model-2)	0.8617	0.7933	0.0828	0.1012	0.6293	0.2383	43.63
3(Model-3)	0.8130	0.6550	0.1061	0.1441	0.6033	0.2342	30.43

3D QSAR

The 3D QSAR analysis of the Benzimidazole derivatives was performed using kNN-MFA method coupled with stepwise forward-backward variable selection method. k-Nearest neighbor molecular field analysis (kNN-MFA) requires suitable alignment of given set of molecules. Molecular alignment was used to visualize the structural diversity in the given set of molecules. The template structure i.e. Benzimidazole was used for alignment by considering the common elements of the series as shown in Fig. 5 and 6.

Table 3: Summary of 3D QSAR Model 1-3

Trials	kNN	DOF	q ²	q ² se	pred_r ²	pred_r ² se
1(Model-1)	2	23	0.8928	0.0933	0.9387	0.0603
2(Model-2)	2	23	0.8125	0.1104	0.9374	0.0785
3(Model-3)	2	23	0.8895	0.0956	0.8226	0.0978

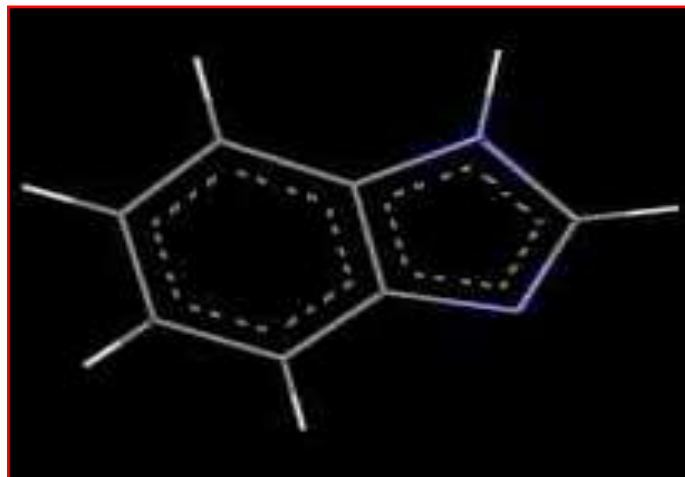


Figure 5: Template molecule of Benzimidazole

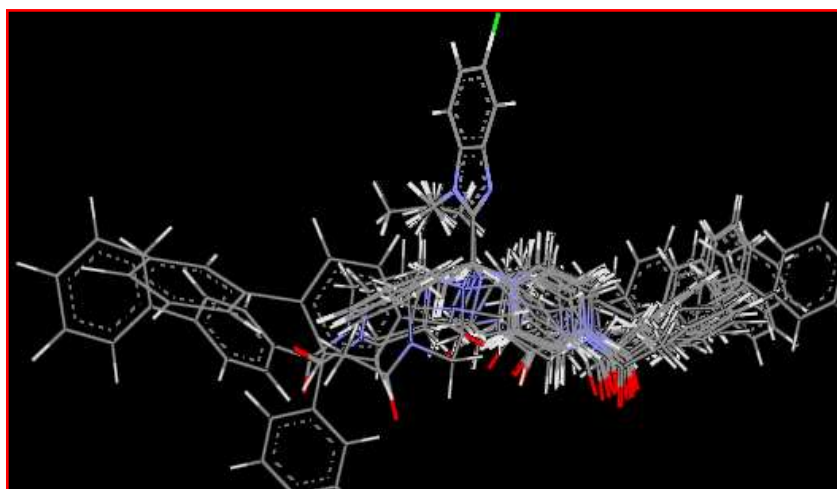


Figure 6: Stereo view of aligned molecules of Benzimidazole

The above aligned molecules have RMSD value within a range ($<2\text{\AA}$). The molecules superimposed on template structure performed by template selection based method that is atom/shape based RMS fit, multifit.

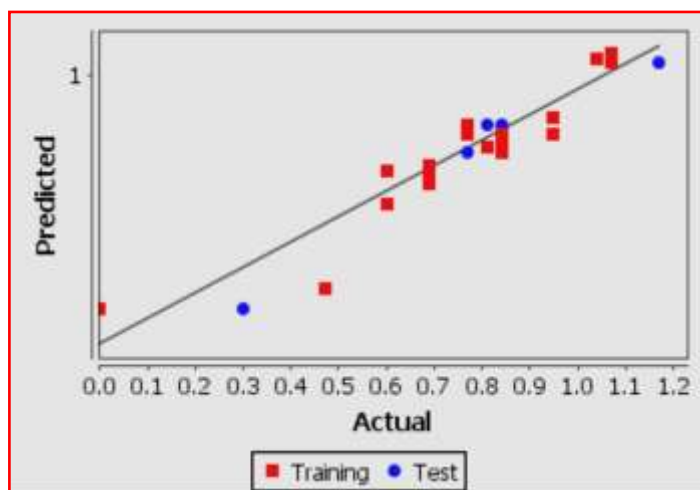


Figure 7: Data fitness plot for model-11

Model (Test set: 11, 12, 13, 18, 19, 2, 20, 21, 28, 3 and 31)

$pIC_{50} = S_{135}$ (-0.1254 -0.1251)

Statistics: [kNN= 2; n = 25; DOF= 23; $q^2 = 0.8928$; $q^2_{se} = 0.0933$; $pred_r^2 = 0.9387$; $pred_r^2_{se} = 0.0603$]

The model explains values of k (2), q^2 (0.8928), $pred_r^2$ (0.9387), q^2_{se} (0.0933), and $pred_r^2_{se}$ (0.0603) prove that QSAR equation so obtained is statistically significant and shows the predictive power of the model is 89.28% (internal

validation) and 93.87%(external validation). Table 6. represents the predicted inhibitory activity by the model for training and test set.

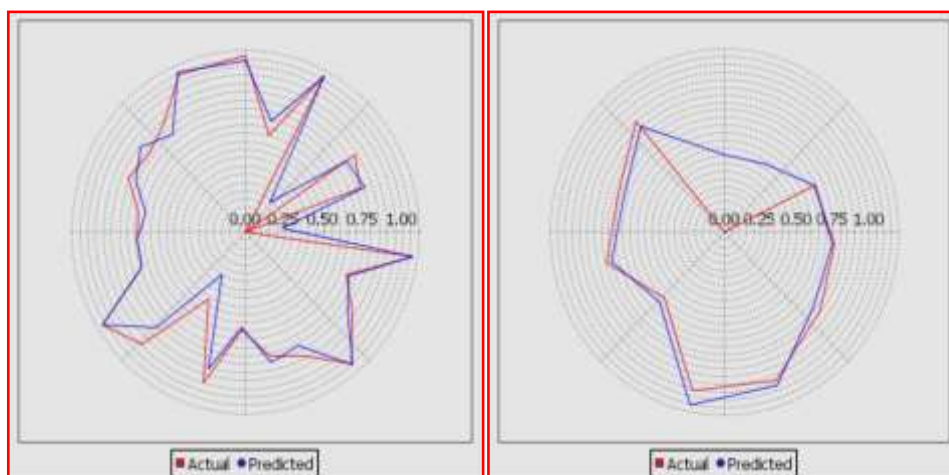


Figure 8: Graph between actual vs. predicted biological activity of training and test set for Model-11

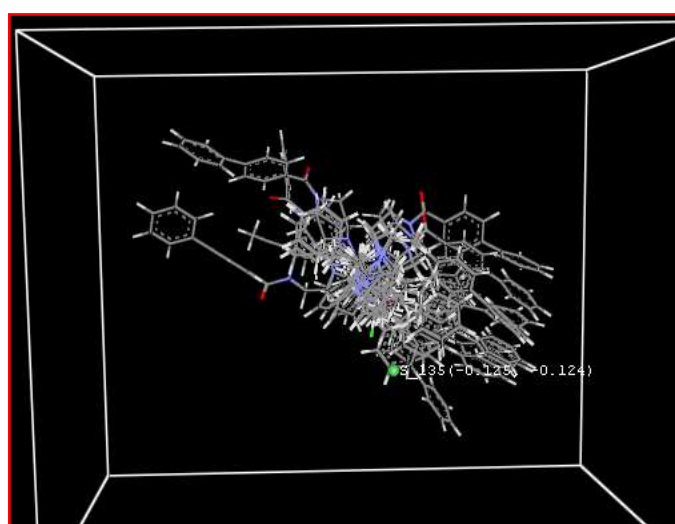


Figure 9: 3D-alignment of molecules with the important steric points contributing model-1 with ranges of values shown in parenthesis

Table 4: Actual and predicted activities for 36 compounds based on the best 2D/3D-QSAR model of Benzimidazole derivatives

Sr. No.	Molecule name	Actual activity at concentration 50ug/ml (Log value)	Predicted activity of 2D model-1	Predicted activity of 3D model-1
1	BPC1	0	0.508747	0
2	BPC2	0.47	0.559161	0.235572
3	BPC3	0.6	0.642872	0.644998
4	BPC4	0.69	0.680039	0.749967
5	BPC5	0.77	0.730453	0.804981
6	BPC6	0.77	0.814164	0.82502
7	BPC7	0.84	0.767456	0.805052
8	BPC8	0.84	0.81787	0.860148
9	BPC9	0.95	0.901581	0.235572
10	BPC10	1.07	1.005511	1.055014
11	BPC11	1.04	1.055925	1.054986
12	BPC12	1.07	1.139636	1.09
13	BPC13	0	0.527822	0
14	BPC14	0.6	0.578236	0.644895
15	BPC15	0.81	0.661947	0.750042
16	BPC16	0.69	0.699114	0.645002

17	BPC17	0.77	0.749528	0.82502
18	BPC18	0.77	0.833239	0.804991
19	BPC19	0.84	0.78653	0.84
20	BPC20	0.84	0.836944	0.805019
21	BPC21	0.95	0.920655	0.860147
23	BPC22	1.04	1.024585	1.055014
23	BPC23	1.04	1.074999	1.07
24	BPC24	1.68	1.15871	1.13
25	BPC25	0.3	0.543184	0.23528
26	BPC26	0.69	0.593598	0.69
27	BPC27	0.81	0.677309	0.84
28	BPC28	0.69	0.714476	0.749958
29	BPC29	0.77	0.76489	0.805052
30	BPC30	0.77	0.848601	0.804988
31	BPC31	0.84	0.801892	0.805052
32	BPC32	0.84	0.852306	0.805009
33	BPC33	0.95	0.936017	0.95
34	BPC34	1.07	1.039947	1.055014
35	BPC35	1.17	1.090361	1.04
36	BPC36	1.15	1.174072	1.11

The data fitness plot for model is shown in Fig. 5 The plot of observed vs. predicted activity provides an idea about how well the model was trained and how well it predicts the activity of the external test set.

Result plot in which 3D-alignment of molecules with the Training set and Test set important steric points contributing in the model with ranges of values shown in the parenthesis represented in Fig.5 It shows the relative position and ranges of the corresponding important steric fields in the model provides guideline for new molecule design as follows-

(a) Steric field, S_{-135} (-0.1254 -0.1251) has negative range indicates that negative steric potential is favorable for increase in the activity and hence less bulky substituent group is preferred in that region.

CONCLUSION

In the present investigation, all proposed QSAR models were statistically significant, thus, from above QSAR investigations it could be concluded that 2D/3D descriptors properties of substitutedbenzimidazole derivatives will show the better antifungal activity. The good correlation between experimental and predicted biological activity for compounds in the test set further highlights the reliability of the constructed QSAR model. The requirements for the more potent biological activity are explored with 2D, 3D and group based QSAR studies. The 2D technique indicates the importance of + 0.3703(ChlorinesCount) +0.6759 (SaaNE-index) + 0.7458 (SaaaCE-index) -4.1531 antifungal activity of the compounds. The 3D QSAR analysis makes it possible to relate chemical structures of ligands and their binding affinity with respect to different bio targets by using the kNN-MFA techniques. Thus it provides a direct view of factors expressed in terms of molecular fields (electrostatic, steric) affecting the binding affinity. This in turn could give the reasonably good prediction of binding affinity. The location and range of function values at the field points selected by the models provide clues for the design of new molecules. Hence, this method is expected to provide a good alternative for the drug design.

ACKNOWLEDGMENT

The author wishes to express gratitude to V-life Science Technologies Pvt. Ltd. Pune, for providing the software for the study. The authors are very thankful to the management of MET's Institute of Pharmacy for their constant support and providing all facilities to complete this work.

Conflict of Interest:

The author declares that they do not have any competing interests.

REFERENCES

1. Ragno R. www. 3d-qsar. com: a web portal that brings 3-D QSAR to all electronic devices—the Py-CoMFA web application as tool to build models from pre-aligned datasets. *Journal of computer-aided molecular design*. 2019 Sep;33:855-64.
2. Castilho MS, Guido RV, Andricopulo AD. 2D Quantitative structure–activity relationship studies on a series of cholesteryl ester transfer protein inhibitors. *Bioorganic & medicinal chemistry*. 2007 Sep 15;15(18):6242-52.
3. Di Santo R, Tafi A, Costi R, Botta M, Artico M, Corelli F, Forte M, Caporuscio F, Angiolella L, Palamara AT. Antifungal agents. 11. N-substituted derivatives of 1-[(aryl)(4-aryl-1 H-pyrrol-3-yl) methyl]-1 H-imidazole: synthesis, anti-candida activity, and QSAR studies. *Journal of medicinal chemistry*. 2005 Aug 11;48(16):5140-53.
4. Baumann K. An alignment-independent versatile structure descriptor for QSAR and QSPR based on the distribution of molecular features. *Journal of chemical information and computer sciences*. 2002 Jan 28;42(1):26-35.
5. Ahire ED, Sonawane VN, Surana KR, Talele GS. Drug discovery, drug-likeness screening, and bioavailability: development of drug-likeness rule for natural products. In *Applied pharmaceutical practice and nutraceuticals* 2021 Apr 14 (pp. 191-208). Apple Academic Press.

6. Shen M, Xiao Y, Golbraikh A, Gombar VK, Tropsha A. Development and validation of k-nearest-neighbor QSPR models of metabolic stability of drug candidates. *Journal of medicinal chemistry*. 2003 Jul 3;46(14):3013-20.
7. Surana KR, Ahire ED, Sonawane VN, Talele SG, Talele GS. Informatics and methods in nutrition design and development. In *Natural Food Products and Waste Recovery 2021* Jul 8 (pp. 33-49). Apple Academic Press.
8. Gramatica P. Principles of QSAR models validation: internal and external. *QSAR & combinatorial science*. 2007 May;26(5):694-701.
9. Surana KR, Ahire ED, Sonawane VN, Talele SG. Biomolecular and Molecular Docking: A Modern Tool in Drug Discovery and Virtual Screening of Natural Products. In *Applied Pharmaceutical Practice and Nutraceuticals 2021* Apr 14 (pp. 209-223). Apple Academic Press.
10. Moorthy NH, Ramos MJ, Fernandes PA. Structural analysis of α -glucosidase inhibitors by validated QSAR models using topological and hydrophobicity based descriptors. *Chemometrics and Intelligent Laboratory Systems*. 2011 Dec 15;109(2):101-12.
11. Ajmani S, Agrawal A, Kulkarni SA. A comprehensive structure–activity analysis of protein kinase B-alpha (Akt1) inhibitors. *Journal of Molecular Graphics and Modelling*. 2010 Apr 1;28(7):683-94.
12. Surana KR, Ahire ED, Sonawane VN, Talele SG, Talele GS. Molecular modeling: novel techniques in food and nutrition development. In *Natural Food Products and Waste Recovery 2021* Jul 8 (pp. 17-31). Apple Academic Press.
13. Ajmani S, Jadhav K, Kulkarni SA. Group-based QSAR (G-QSAR): mitigating interpretation challenges in QSAR. *QSAR & Combinatorial Science*. 2009 Jan;28(1):36-51.
14. Alderton WK, Cooper CE, Knowles RG. Nitric oxide synthases: structure, function and inhibition. *Biochemical journal*. 2001 Aug 1;357(3):593-615.
15. Lounnas V, Ritschel T, Kelder J, McGuire R, Bywater RP, Foloppe N. Current progress in structure-based rational drug design marks a new mindset in drug discovery. *Computational and structural biotechnology journal*. 2013 Feb 1;5(6):e201302011.
16. Bailey D, Zanders E, Dean P. The end of the beginning for genomic medicine. *nature biotechnology*. 2001 Mar;19(3):207-9.
17. Keter FK, Darkwa J. Perspective: the potential of pyrazole-based compounds in medicine. *Biometals*. 2012 Feb;25:9-21.
18. Clark M, Cramer III RD, Van Opdenbosch N. Validation of the general purpose tripos 5.2 force field. *Journal of computational chemistry*. 1989 Dec;10(8):982-1012.
19. Cochran FR, Selph J, Sherman P. Insights into the role of nitric oxide in inflammatory arthritis. *Medicinal Research Reviews*. 1996 Nov;16(6):547-63.
20. Cramer RD, Patterson DE, Bunce JD. Comparative molecular field analysis (CoMFA). 1. Effect of shape on binding of steroids to carrier proteins. *Journal of the American Chemical Society*. 1988 Aug;110(18):5959-67.
21. de Béthune MP. Non-nucleoside reverse transcriptase inhibitors (NNRTIs), their discovery, development, and use in the treatment of HIV-1 infection: a review of the last 20 years (1989–2009). *Antiviral research*. 2010 Jan 1;85(1):75-90.
22. Spyralis F, Cozzini P, Kellogg GE. Applying computational scoring functions to assess biomolecular interactions in food science: Applications to the estrogen receptors. *Nuclear receptor research*. 2016;3.
23. Halgren TA. Merck molecular force field. I. Basis, form, scope, parameterization, and performance of MMFF94. *Journal of computational chemistry*. 1996 Apr;17(5-6):490-519.
24. Halgren TA. Merck molecular force field. II. MMFF94 van der Waals and electrostatic parameters for intermolecular interactions. *Journal of Computational Chemistry*. 1996 Apr;17(5-6):520-52.
25. Kennedy GG, Dimock MB. 2-Tridecanone: A natural toxicant in a wild tomato responsible for insect resistance. In *Natural Products 1983* Jan 1 (pp. 123-128). Pergamon.
26. Jain AN. Scoring functions for protein-ligand docking. *Current Protein and Peptide Science*. 2006 Oct 1;7(5):407-20. I. M. Kapetanovic, *Chemico-Biological Interactions*, 171, 165–176(2008).
27. Zhan P, Liu X, Li Z. Recent advances in the discovery and development of novel HIV-1 NNRTI platforms: 2006-2008 update. *Current medicinal chemistry*. 2009 Aug 1;16(22):2876-89.